MANUFACTURING AND CHARACTERIZATION OF POLY (LACTIC ACID)/CARBON BLACK CONDUCTIVE COMPOSITES FOR FDM FEEDSTOCK:

AN EXPLORATORY STUDY

Dylan Fitz-Gerald, Justin Boothe

Advisor: Dr. Linda Vanasupa

June, 2016

Table of Contents

1 Abstract

This exploratory study developed methods of manufacturing and characterizing the electrical properties of small batches of conductive composite feedstock for the Fused Deposition Modeling (FDM) manufacturing process, commonly known as 3D printing. We utilized a solution casting process of Poly(lactic acid) (PLA) (Grade 4043D, NatureWorks, LLC.) and Carbon Black (CB) (Vulcan® XC72, Cabot Corp.) in chloroform. The resulting composite precursor was cryogenically treated with liquid nitrogen and milled in a coffee grinder in order to achieve particles that could be fed into the extruder. Composite precursors were dried in a vacuum oven at an elevated temperature of 38°C. Filaments were produced via filament extruder (Filastruder 2.0). Volume resistivity was measured using a modified method of ASTM D991-89 with a customized test fixture. Compositions ranging from 0.1 to 45 vol% of CB were manufactured in this way. Results indicated that compositions of 25 vol% and 30 vol% CB showed regions of conductivity in the filament, however their conductivities were highly inconsistent, with lengths of filament having both conductive and nonconductive regions. Regions that did conduct were ohmic, with volume resistivities ranging from 1.4 to 63 * 10^{-2} ohm*m. Samples with concentrations of 35 vol% and greater were unable to be extruded effectively due to the limitations of the equipment available.

2 Motivation for Research

In the course of our studies, we noticed a dark area in the collective research available pertaining to the combinations the fields of study of functional electronic materials (including conductive composites) and rapid prototyping manufacturing techniques (such as the Fused Deposition Modeling, or “3D Printing”, technique). The research that is available indicates that these materials have great potential for novel applications, and as it stands, this technology can already be utilized to produce a wide variety of specialized sensors inexpensively and at home with consumer available FDM printers. Conductive feedstocks for 3D printing are already available through companies such as ProtoPlant Inc., which, aside from their obvious applications as simple conductive pathways, can also be used for producing fully realized products with built in strain gauges, capacitive touch sensors, liquid level indicators, and more.

We believe that being able to reliably produce 3D printable conductors and understand their nature are among the first steps in a long road to developing other functional electronic materials for 3D printing, and that this technology could be the key to a new and exciting world of manufacturing and technology.

3 Literature Review

3.1 Introduction

Fused Deposition Modeling (FDM) (also known as Fused Filament Fabrication (FFF)) is a rapid prototyping process traditionally in which thermoplastics or waxes are extruded layer-by-layer into a modeled shape. Much of the consumer FDM units are typically designed to utilize a filament feedstock of either or both acrylonitrile butadiene styrene (ABS) and Poly (lactic-acid) (PLA), however a wide array of functional materials are being developed and are entering the market.[1, 2]

The polymer poly (lactic acid) is typically a blend of enantiomers, L- and D-lactic acid. The ratio of L- and D- types determine the chemical characteristics of the final plastic, making the properties tunable. PLA has the benefit of being biodegradable. The raw lactic acid is typically derived from the fermentation of corn and other starches, which is processed into polymers primarily by the company NatureWorks LLC in the United States. [3, 4, 5]

Carbon black (CB) is a general term for types of ultrafine paracrystalline carbon particles (10-400 nm diameter), usually with a very high surface area to volume ratio, typically produced through the incomplete combustion of petroleum tars. It is distinct from soot and other combustion byproducts in that carbon black is composed nearly entirely of elemental carbon (90-99% carbon, 0.1-10% oxygen, 0.2-1.0% hydrogen, with small amounts of sulfur and ash), whereas other combustive byproducts may contain large amounts of ashy compounds. Most commonly, it is used as a pigment and reinforcing phase for polymers, notably automobile tires and other rubbers, accounting for nearly 90% of its consumption. Carbon black is desirable as a filler in polymers since it is generally heat resistant, UV absorbent, chemical resistant, has a low density and low thermal expansion, and acts as an antiabrasive. Additionally, it is conductive, which allows it to be used in static dissipative and radiation shielding applications.[6, 7]

3.2 Mechanism for Conduction

The mechanism for bulk conductivity in composites, especially those composed of a dispersion of conductive particles in an insulating matrix, seems to be a combination of quantum events and mechanical interactions between particles. The mechanical interactions seem to behave according to percolation theory, which can describe the behavior of connected clusters dispersed randomly in some matrix, in which some property probabilistically emerges after concentration reaches some critical value (the percolation threshold). In the case of PLA/CB composites, the percolation threshold of conductivity is some volume percent concentration of carbon black particles in which the bulk composite transitions from being an insulator to a conductor. In a 2014 study on the electromagnetic shielding potential of a foamed PLA/CB conductive composite, the percolation threshold was estimated to be 1.5 vol.%, as at that point, the resistivity of the composite dropped considerably. This study used Ketjenblack EC-300J carbon black and a casting grade PLA (3052D from NatureWorks LLC). As mentioned before, carbon black can have different morphologies which affect conductivity and different grades of PLA have different properties, so this percolation threshold may not be consistent for all PLA/CB composites. [7, 8, 9, 10]

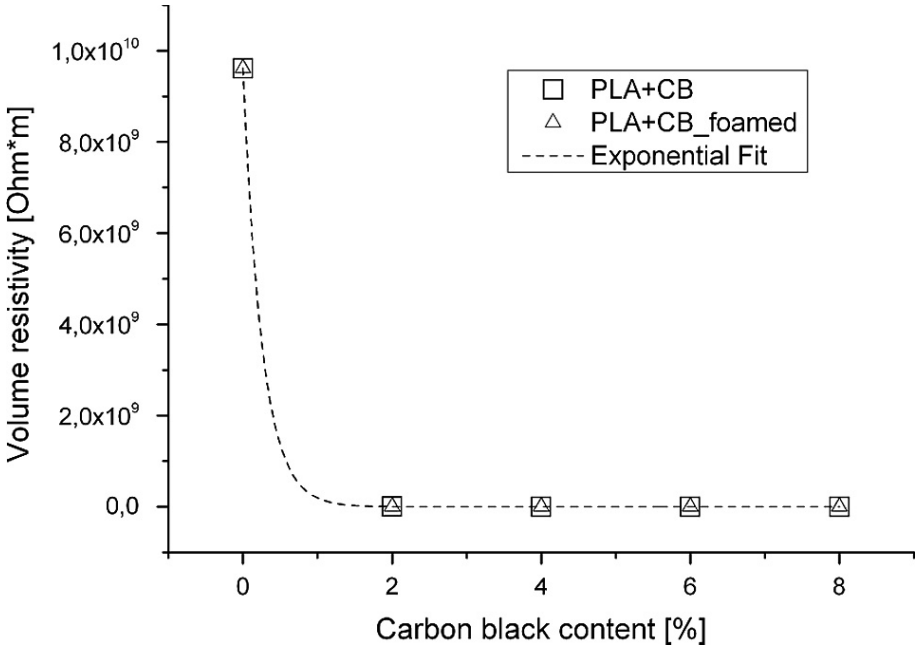

Figure 1: Volume resistivity measure of PLA 3052D from NatureWorks LLC and Ketjenblack EC-300J carbon black (CB) from Akzo Chemicals. Note the sudden decrease of resistivity 1.5 vol.%, which is estimated to be the percolation threshold. Image from: Frackowiak, et al, 2015[8]

Percolation theory is a valuable tool to describe various phenomenon in heterogeneous systems. It was originally developed to describe connection patterns in some continuous, closed packed bonding lattice, say, of perfect conductors and perfect insulators, in which each site is given some probability of being a conductor or insulator. At some critical bond probability (the percolation threshold), conductive paths throughout the entire lattice are highly probable and the conductivity of the lattice becomes finite. If each conductor had some finite resistivity, conductivity of the bulk would therefore increase if concentrations were increased above that threshold concentration. The conductivity of the composite near the conductor-insulator transition point could then be approximated with some percolation equation for conductivity (Eq. 1), where the conductivity σ of the heterogeneous mixture as the volume fraction of the conductive phase Φ exceeds the minimum threshold to establish conductivity Φ_c. The exponent, *t*, is a critical exponent based not on the morphology of the system, but instead on the dimensionality of the system (thus, *t* should be within 1.65 to 2.0 for 3D systems).[9, 10]

$$\text{(Eq. 1) } \sigma \propto (\Phi - \Phi_c)^t;\ \Phi \to \Phi_c^+$$

Unfortunately, percolation theory itself does not seem to work well enough to completely characterize conductive composites. First, it typically applies only in randomly distributed closed packed systems near the percolation threshold, which is not always the case for binary composite systems. Values of *t* should theoretically be within the range of 1.65 to 2.0, however they have been measured as high as 3.1 for graphite particles in polymers or even 4.0 (although this can be presented as an argument that tunneling is necessary to account for these values). Although percolation theory does not model the system well, it is important that it establishes the precedent that some critical concentration of the components of binary systems exists where properties such as conductivity will emerge. [10]

Conductivity is better described using effective media theories (EMT), which are based on three cases of high conductivity and low conductivity phases. In Bruggeman's symmetric medium, the conductive medium is filled with the low conductivity phase at some volume ratio. In Bruggeman's asymmetric medium, the low conductivity phase are uniformly coated particles in the conductive medium. The general effective media (GEM) is assumed to be an intermediate system in which neither phase completely coats another. The equation for the GEM can be simplified to the form of percolation theory (Eq. 2), where σ_m is the conductivity of the medium, σ_h is the conductivity of the high-conductivity phase, Φ and Φ_c are again the volume fraction of conductive phase and the critical volume fraction, respectively, and t' is an exponent related to the critical volume fraction and the shape of the grains, where m_h is some coefficient related to the morphology of the grains (Eq. 3). [9, 10]

$$\sigma_m = \sigma_h \left(\frac{\Phi - \Phi_c}{1 - \Phi_c}\right)^{t'} \quad \text{(Eq. 2)}$$

$$t' = m_h \Phi_c \quad \text{(Eq. 3)}$$

The GEM equation is better at approximating the properties of composites over the percolation equation, primarily because GEM takes into account the morphologies of the phases, whereas percolation theory assumes regular lattices. Furthermore, GEM could be used to predict the percolation threshold based on the morphologies of the phases and their properties. [9, 10]

Both percolation and the effective media theories rely on conductivity through networks of physically contacting particles in order to establish electrical continuity, which is infeasible for sufficiently large objects with relatively small percolation thresholds. This discrepancy is attributed to the quantum effects of tunneling and hopping, where conductivity can occur between sufficiently close particles, despite being separated by an insulating medium. While it can be assumed that the conductivity of a composite is due to a combination of percolation and quantum effects, percolation has a far greater influence on the final properties as tunneling and hopping will not occur if the particles are too greatly spaced. [9, 10]

3.3 Electrical Properties

A material is Ohmic if the relationship of the Current and Voltage is a linear fit and follows Ohm's law. In similar electrical systems, such as an epoxy composite with carbon nanoparticles, there is region of Quasi-Ohmic behavior that one could expect to see in our similar system. In another similar study a material system of silicone and Carbon Black a similar result occurred resulting in a very linear Ohmic relationship as seen in Figure 2.[11, 12]

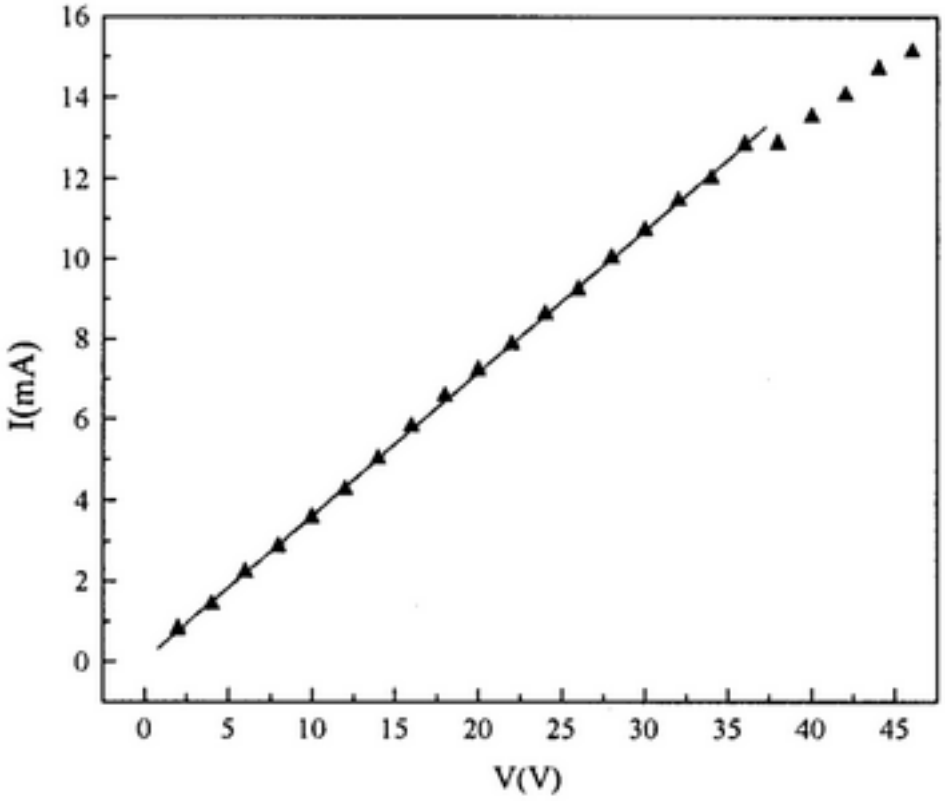

Figure 2: I-V characteristic of conductive silicone rubber with 30 wt % Carbon Black showing that at most voltages the conduction is Ohmic. Sau, et al, 1997.[13]

The piezoresistive effect is the change in electrical resistance when mechanical strain is applied. The piezoresistive effect has been discovered in the silicon carbon black system along with other similar systems. Some explanation for the piezoresistance in some systems is that when stress or strain is applied conductive network is changed which results in a change of the electrical conductivity (Figure 3). [13]

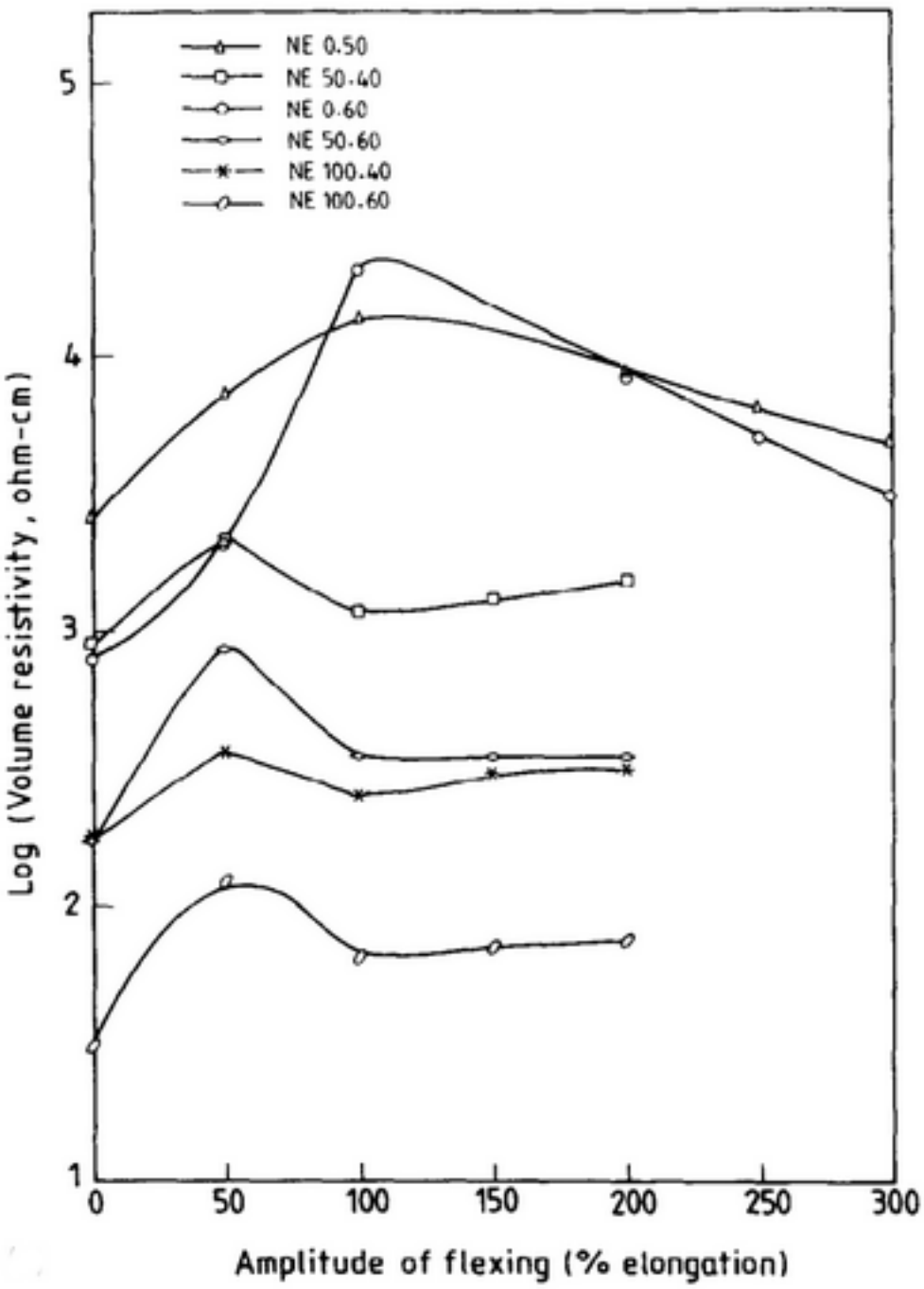

Figure 3: This graph represents the change in Volume Resistivity over the percent elongation which shows how the conductive networks break down in this sample of nitrile rubber in a 50/50wt% blend with Carbon Black. Image from: Sau, et al, 1997.[13]

After peaking at around 50% elongation the resistivity levels out at 100% then remains constant showing that once the conductive network is sufficiently broken down at a certain point it is no longer effected. The change in conductivity depends on several factors including: percent elongation, the frequency of stress-strain cycles, and the total number of cycles. This is because

in a polymer with a conductive matrix it is theorized that the breakdown of the conductive network occurs for a number of cycles before stabilizing, this can be seen in Figure 4.

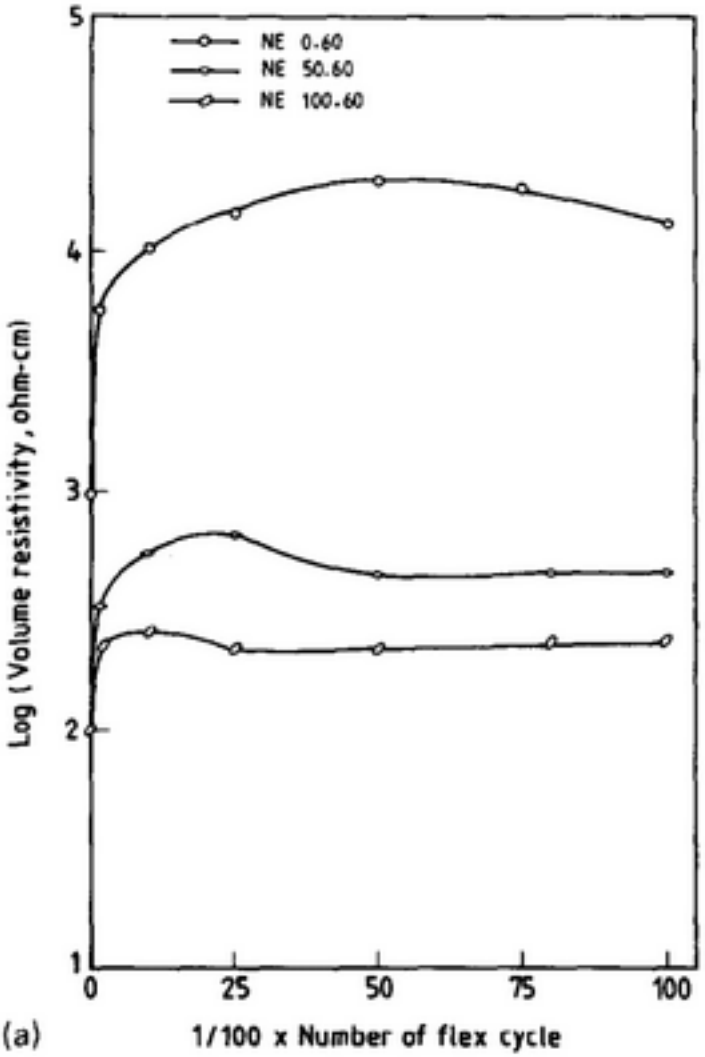

Figure 4: When the material is being put under cyclic stress there is a breakdown of the conductive paths after about 2500 cycles under an applied load. Image from: Sau, et al, 1997.[13]

This effects the piezoresitive effect because the applied stress breaks down the network, but as the stress is removed new networks are created.

In terms of 3D printed properties there are several different factors that will affect the resistivity of the system. In the PLA/CB system the resistance can change depending on if the measuring is done in the same plane as the layers or vertically through each layer. The difference can be seen in the data produced by ProtoPasta's PLA/CB filament measurements[2]:

Volume resistivity of 3D printed parts perpendicular to layers: 30 ohm-cm

Volume resistivity of 3D printed parts through layers (along Z axis): 115 ohm-cm

There will be a large range of possibilities of the volume resistivity due to the possible print parameters of any 3D printer. The adhesion between layers likely influences the volume resistivity, and this can be modified by changing the printing temperature and layer thickness. Therefore, a test of the volume resistivity of a 3D system is highly dependent on the specific printer and its settings and acts better as a baseline that a source of accurate data. However, by finding the relationship between different printer parameters and the resistivity it might be possible to predict the electrical properties of the material based on the way it was printed.

3.4 Predictive Modeling

An important part of designing products is being able to model the properties of the materials. As mentioned before, the bulk conductivity of 3D printed PLA/CB composite from ProtoPlant is anisotropic with respect to layer orientation, however no models of this conductivity phenomena have been made. Models have been made, however in order to predict the mechanical properties of 3D printed materials, which may shed some light on these effects.[2]

Attempts at modeling expected mechanical behaviors of FDM manufactured ABS P400 have been by two distinct entities: Li (et. al) and Rodriguez (et al). Li first implemented a model which assumes printed layers behave like a composite lamina, with each lamina in this case composed of overlapping ellipsoid filaments with some void density, which would then be expected to behave according to lamination theory. Similarly, Rodriguez assumed that the voids could be considered as some unit cell of a periodic body, thus the orthotropic properties could be predicted using a simplified mechanics of materials approach (Figure 6). Both models were able to somewhat predict the expected trends in mechanical properties, however not very accurately.[14, 15, 16, 17]

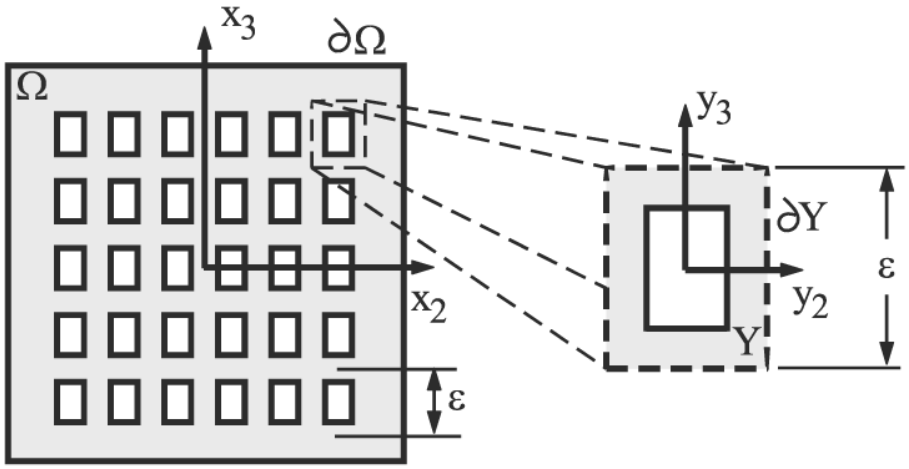

Figure 5: Periodic body and unit cell approach to predicting the mechanical properties of FDM manufactured ABS, as used by the Rodriguez (et al.) mechanics approach. Image from: Rodrı´guez, et al, 2003.[17]

Li later modeled the filament adhesion of the ABS as if they were sintering particles (Figure 7). It was then determined that under the circumstances of FDM, the bonds would be significantly weaker than the bulk ABS, thus attributing to the inaccuracies of the previous models. The "effectiveness" of the bonds between strands are highly temperature dependent, thus the neck

size and formation speed would increase with temperature. Although the neck formation would increase, mechanical properties and print quality would not necessarily increase with temperature, as thermal degradation and issues with dimensionality may occur, as supported by a study on the compressive behavior of FDM manufactured iron-ABS composites, which attribute lowered mechanical properties in part to residual stresses caused by the thermal cycling of subsequent layers.[16, 18]

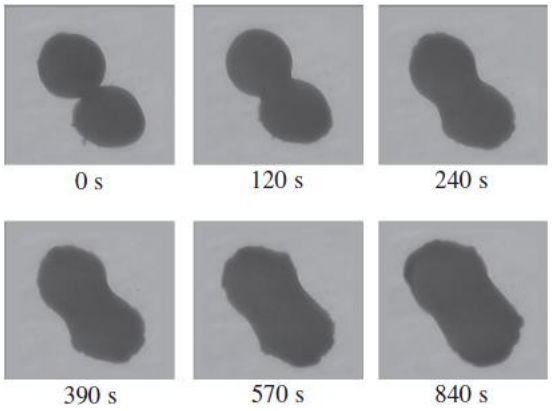

Figure 6: Neck Growth evolution for extruded ABS P400 fibers 0.47mm in diameter at 200°C. Image from: Li, et al, 2002.[15]

These models only attempt to predict the behavior of a pure ABS P400, and not composite materials. For example, they may not accurately describe the interlaminar melt behavior, as the models (noted by Li) assume that the coefficient of thermal conductivity must remain relatively constant. In experiments on metallic ABS composites with iron and copper particles, thermal conductivity becomes nonlinear with respect to temperature at high fill volumes (Figure 8). This is attributed to some percolation effect with establishing thermally conductive pathways as affected by the differences in thermal expansion between the metallic particles and the ABS matrix.[19, 20]

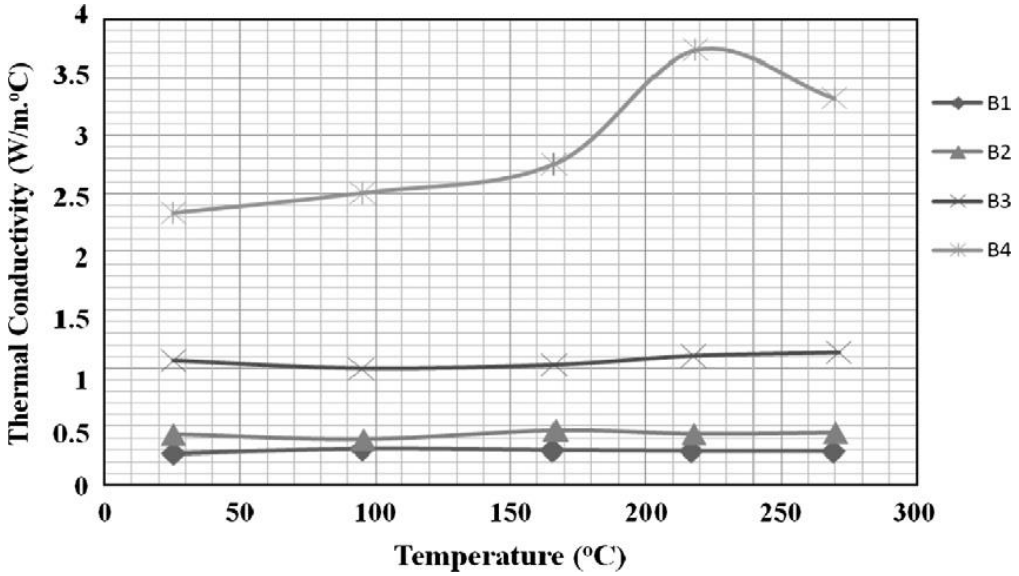

Figure 7: Thermal conductivity of copper-filled ABS composites at various temperatures. Sample filler loading: B1 at 5%, B2 at 10%, B3 at 20%, B4 at 30%. Image from: Nikzad, et al, 2011.[19]

Another important aspect for modeling the electrical behavior of conductive composites is the distribution of particles during melt flow at extrusion. Nikzad (et. al) modelled the melt flow of an ABS-iron composite at the extrusion tip using flow analysis software. They noted that composite experienced non-Newtonian flow behavior at the typical extrusion temperature of 270°C, as well as a velocity maximum at the very center of the melt flow (Figure 9). Pegel (et al.) studied the dispersion of multiwalled carbon nanotubes (MWNT) in a polycarbonate matrix for injection moldable conductive composites, which measured that the factors with the largest effects on conductivity are the injection velocity and melt temperature. High injection velocities caused a high degree of strand alignment and separation (especially along the skin of the molding), thus lowering conductivity as they did not allow networks to form. High injection temperatures also lowered conductivity as the strands were more likely to tangle and agglomerate and not form secondary conductive networks. Although the effects of melt flow on carbon black particles have not been studied on PLA/CB composites, it seems likely that there will be some effect on particle dispersion due to the FDM processing.[19, 20, 21, 22]

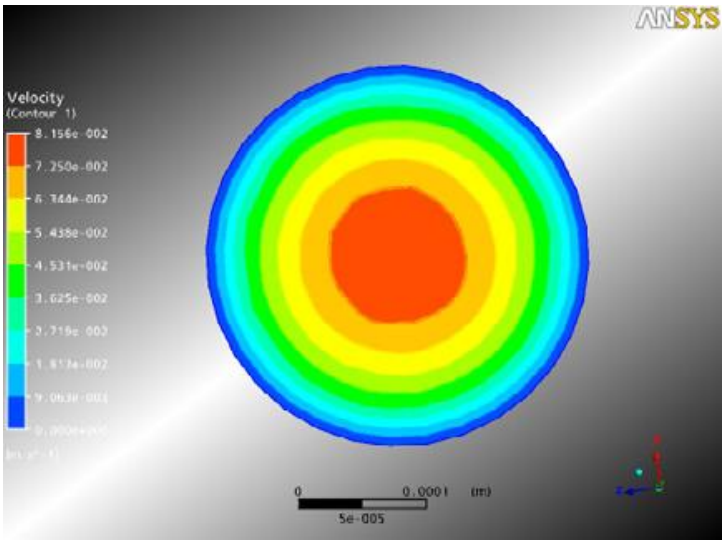

Figure 8: Melt velocity at extrusion tip of ABS/Iron composite during FDM manufacturing. Image from: Nikzad, et al, 2009.[20]

4 Experimental

4.1 Materials and Methods

4.1.1 Materials and Equipment

The materials used for the matrix and conductive filler, respectively, were Grade 4043D Poly(lactic acid) (NatureWorks, LLC) and Vulcan® XC72 Carbon Black (Cabot Corporation). Grade 4043D Poly(lactic acid) (NatureWorks, LLC) was chosen for the matrix material, as it is an extrusion grade PLA commonly used for 3D printer feedstock as well as the PLA used in the Electrically Conductive PLA 3D Printer Filament sold by ProtoPlant INC.[2], and Vulcan® XC72 Carbon Black (Cabot Corporation) was chosen for the conductive filler as it promised "a full range of conductivity performance… at lower loadings than other XC carbon blacks or standard carbon blacks"[23] and was readily acquirable.

During precursor preparation, Anhydrous chloroform (≥ 99.5%, C2432 Sigma-Aldrich) was utilized as a solvent for the PLA during precursor preparation, as, out of all solvents capable of dissolving PLA, it was determined to be the safest to regularly handle with the laboratory and safety equipment available. For glassware, Kerr® 8oz Wide Mouth Half Pint Jars were utilized as they were inexpensive, durable, and could readily resist solvent attack. PTFE (Polytetrafluoroethylene) film (SLICK™ SHEET) was also utilized during precursor preparation, as PTFE resists chloroform attack and acts as a nonstick surface.

Electrical testing utilized a Hewlett Packard 6186C DC Current Source and an Agilent 3405A 5½ Digital Multimeter as well as a custom-made test fixture.

4.1.2 Precursor Preparation

Samples of varying carbon black (CB) composition in PLA were prepared (0.1, 0.5, 1, 5, 10, 20, 25, 30, 35, 40, and 45 vol% CB). First, the raw PLA pellets were dried in a vacuum oven at -0.07 MPag and 38℃ (~100°F) for 24 hours to drive off moisture absorbed from the atmosphere. Due to the relatively large particle size of the PLA pellets (compared to the fine CB powder), roughly 20 grams of PLA were measured using a high precision electronic balance, then utilizing this "actual" mass value of PLA, the required amount of CB to reach the correct concentration was then calculated using the densities provided by the suppliers[23,24] using a modified version (Eq. 5) of the volume percent calculation (Eq. 4) (where V is the volume of each component, ρ is the reported density in g/cm^3, m is the mass in grams, and Vol% is the decimal value of desired concentration), with an allowable tolerance of ±1% of the calculated mass value.

$$\text{(Eq. 4)} \qquad Vol\% = \frac{V_{CB}}{V_{CB} + V_{PLA}}$$

$$\text{(Eq. 5)} \qquad m_{CB} = \frac{(m_{PLA}\rho_{PLA})(Vol\%)}{\rho_{CB}(1-Vol\%)}$$

The PLA and CB were added to 150mL of chloroform in a jar, which was sealed and stirred with a magnetic mixer and stir bar for 24 hours under a fume hood to ensure complete dissolution of the PLA and sufficient distribution of the CB. It was noted that the carbon black tended to statically "cling" to the weigh boat, so, in order to assure accurate concentrations, the weight boat was measured before and after adding the CB to the chloroform. After mixing, the solution was poured onto a PTFE sheet, allowing chloroform to evaporate off for 24 hours under a fume hood.

The resulting film was cut into smaller strips using scissors, which were cryogenically treated with liquid nitrogen and milled in a coffee grinder in order to produce small particles of precursor.

During the cryogenic treatment, it was noted that frost would formed on the precursor. In order to remove moisture that would possibly absorb into the precursor, each sample was dried in a vacuum furnace under -0.07 MPag at 38℃ (~100°F) for 24 hours. Dried precursor samples were then stored in sealed in sealed jars with added silica desiccant packages to prevent moisture absorption in the time between vacuum drying and filament extrusion.

4.1.3 Filament Extrusion

The extruder used to generate the feedstock was a Filastruder 2.0, a product intended for hobbyists to make their own custom batches 3D printer feedstock, and implements a single-screw auger to feed material into a heated die, 1.75mm in diameter. For each sample, the extruder was set to a die temperature of 170℃, which is a temperature supported by reports given of other Filastruder users and was verified as a reasonable temperature empirically.

Due to the design of the extruder, the relatively small amounts of precursor generated were insufficient to extrude by themselves in any meaningful amount, as there was insufficient material for the auger to "push" through the die. To cope with this, raw PLA pellets were first added to "prime" and clear the barrel before adding the precursor. After the hopper was empty of precursor, the hopper was then backfilled with raw PLA to "push" the sample through the extruder. The filament produced near these transitions between sample and raw PLA were removed.

4.1.4 Characterization of Electrical Properties

Volume Resistivity was measured using a modified method of ASTM D991-89[25] with a customized test fixture. The fixture holds a section of produced filament and impressed a current through the sample, and measures the subsequent voltage drop over a fixed distance of 10cm (Figures 9, 10).

Figure 9: Test fixture designed with regards to ASTM D991-89

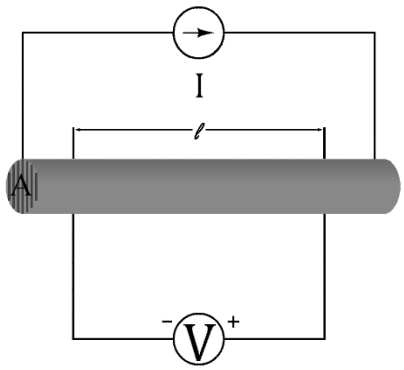

Figure 10: Simplified wiring diagram of test fixture (Figure 9).

The voltage drop was recorded after varying the impressed amperage from 1-10mA by increments of 1 mA, then from 10-100mA by increments of 10mA until failure of the sample from thermal runaway. Due to the small amounts of viable filament feedstock produced, these tests could only be repeated four times for each concentration.

Using graphical analysis of this results, the resistivity, *R*, of each sample could be calculated via the linear best-fit line of the data, due to the linear relation of current and voltage according to Ohm's Law. Using the calculated value for sample resistance, *R*, the gauge length, *l*, and the cross sectional area of the sample, *A*, the volume resistivity of the sample was calculated using the equation for volume resistance provided in ASTM D991-89[25] (Eq. 6). This assumes that the samples are Ohmic (defined here as having an r^2 value greater than 0.95 on the linear best fit line of current vs voltage drop), have a uniform cross sectional area (equal to the average value calculated using the diameter of the cylinder measured using a micrometer), and are completely homogenous in composition.

$$\rho = \frac{RA}{l} \qquad \text{(Eq. 6)}$$

4.1.5 Microscopy of Prepared Samples

For the purpose of understanding the degree of porosity and homogenization of conductive samples in the extruded samples, reflective optical microscopy was performed. Samples were mounted in both transverse and longitudinal directions in cold-mounted acrylic mounts and were subsequently sanded and lightly polished with 2-micron diamond abrasive.

4.2 Results and Discussion

4.2.1 Initial Findings of Experimentation

In the process of extruding the samples, those with carbon black concentrations of 35 vol% and greater were unable to be sufficiently extruded using the Filastruder 2.0 due to being highly viscous at the chosen extrusion temperature, as well as any temperature below the degradation temperature of the PLA. It was also found that the samples with carbon black concentration of 20 vol% and lower were generally nonconductive and could not be measured using the electrical

test parameters. Therefore, data could only be gathered from two concentration levels, 25 and 30 vol%.

Within the extruded samples that could be measured for conductivity, the lengths of filament were highly variable, and had regions both that were conductive as well as non-conductive. The conductive regions of these samples had high surface roughness, high porosity, and were fragile (due to the porosity).

4.2.2 Characterization of Electrical Properties

The resistance was calculated from the slope of the I vs V diagram generated for each sample (Figure 11, 12). Each set of data was fit linearly with an $R^2 \geq .95$, showing that the relationship can be described as linear, thus the sample must be ohmic.

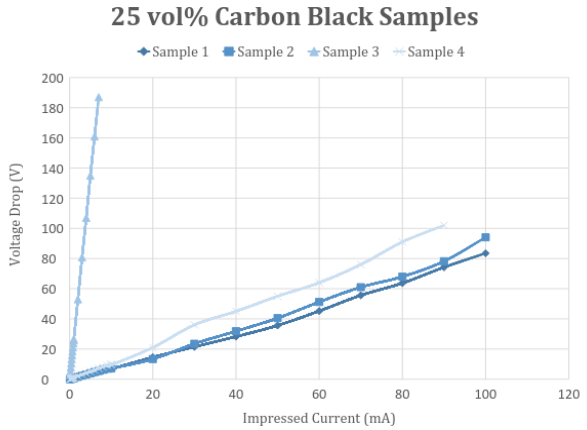

Figure 11: I/V diagram generated for 25 vol% CB filament.

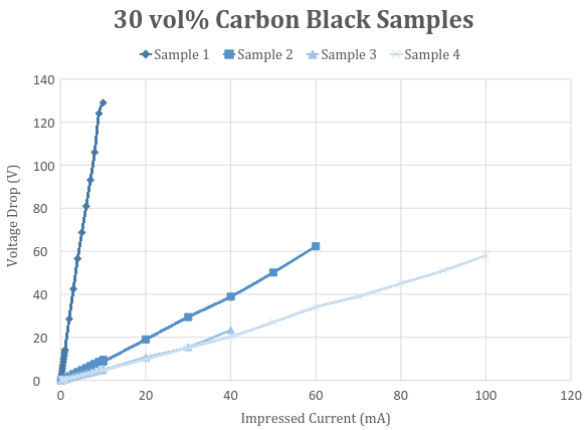

Figure 12: I/V diagram generated for 30 vol% CB filament.

In order to calculate volume resistivity (ρ) of the samples, filament geometry was simplified to a perfect cylinder 10cm long (l) with a cross-sectional area (A) calculated from the average diameter of the sample, using the following equation 6 above. The samples had a wide range of variance in the calculated resistance between samples (Table I).

According to one-way analysis of variance (ANOVA), there is no statistical difference between the volume resistivity of samples belonging to each of the concentration groups (P=0.6388). Removing the two calculated values that seem uncharacteristically high (64.2 Ωcm and 32.1 Ωcm for the 25 and 30 vol% samples, respectively), there is still no significant difference between sample concentration groups (P = 0.2109).

Table I: Summary of Results of Electrical Testing			
CB Concentration	Sample	R (Ω)	ρ (Ωcm)
25 vol%	1	806	2.1
	2	883	2.3
	3	26825	64.2
	4	1120	2.9
30 vol%	1	13267	32.1
	2	1011	2.5
	3	557	1.4
	4	568	1.5

4.2.3 Microscopy of Samples

Micrographs of conductive and nonconductive regions of the 25 and 35 vol% samples were taken using reflective light microscopy at 50x magnification with samples mounted in an acrylic resin. Conductive regions (Figure 13) tended to have high concentrations of pores, while the nonconductive regions (Figure 14) appeared homogenous. Note that the white areas of the conductive sample are due to particles of the acrylic cold-mount filling the pores during the sanding and polishing process.

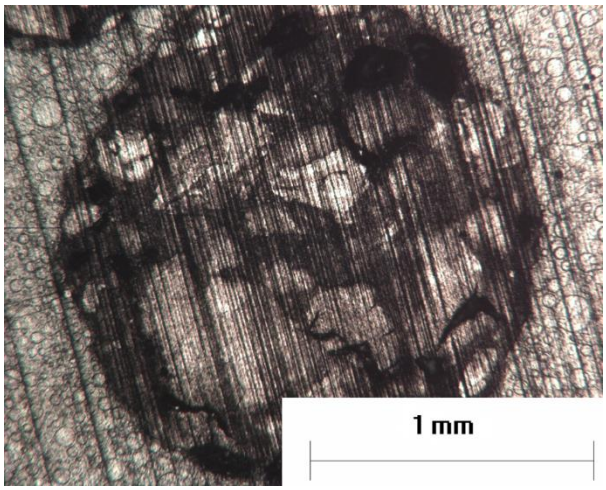

Figure 13: Conductive region of 25 vol% CB/PLA extruded filament.

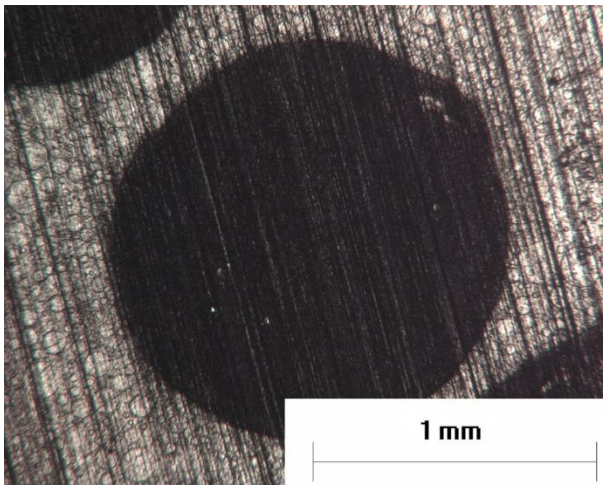

Figure 14: Non-conductive region of 25 vol% CB/PLA extruded filament.

While it may seem counterintuitive that the porous regions have superior conductivity, the exact mechanism behind the correlation between conductivity and porosity is unknown. It is suspected to be caused by chloroform retained in the carbon black during the solvent casting process, where the PLA acts as a barrier to chloroform evaporation during vacuum drying, later forming bubbles as the PLA liquefies during the extrusion. This would be supported intuitively, as regions of the precursor containing greater amounts of carbon black would also release greater amounts of chloroform gas. It should also be noted that even at relatively low loadings of carbon black (as low as 1 vol%), the composite precursors are pigmented a deep black. If it were the case that only regions of relatively high carbon black content are conductive, then either the critical percolation concentration for conductivity of this particular PLA and carbon black grade is significantly higher than 25 vol%, or this specific precursor manufacturing process is highly susceptible to agglomeration.

Regardless, the porosity itself is detrimental to the mechanical properties of the filament and may attribute to the variance in electrical properties, and thus is undesirable. Furthermore, the variance in the filament is proof that the manufacturing process cannot adequately distribute the carbon black evenly throughout the PLA matrix.

4.3 Conclusions

From this exploratory study, the following conclusion can be made:

This combination of PLA and carbon black grades can produce conductive composites which can be extruded into filament feedstock for FDM. While this technically fulfills the primary motivation for research, the produced filament is inadequate for practical use.

While there may be a percolation threshold for conductivity between concentrations of 20 and 25 vol% carbon black according to the electrical testing of produced filament, this estimated range may be unduly influenced by the presence of retained chloroform and the gross agglomeration of carbon black.

Utilizing this solvent casting process and base materials combination allows for a window of utilizable concentrations between 25 and 35 vol% carbon black, where conductive samples can both be manufactured and extruded into filament.

Unfortunately, this methodology produces a highly inconsistent product with severe issues with porosity. Furthermore, this methodology is not readily scalable as throughput is slow (taking three days to produce each sample) and requires the use of a large amount of chloroform, which is expensive and a potential health hazard.

5 References

1. Leig, S. J., Bradle, R. J., Purssel, C. P., Billso, D. R., & Hutchin, D. A. (2012). A Simple, Low-Cost Conductive Composite Material for 3D Printing of Electronic Sensors. *PLoS ONE*
2. Proto Plant. (2015). *http://www.proto-pasta.com/products/conductive-pla*. Retrieved from http://www.proto-pasta.com/: http://www.proto-pasta.com/products/conductive-pla
3. Chemical Sciences Roundtable, B. o. (2001). Commodity Polymers from Renewable Resources: Polylactic Acid. In P. R. Gruber, *Carbon Management: Implications for R&D in the Chemical Sciences and Technology: A Workshop Report to the Chemical Sciences Roundtable.* Washington DC: National Academies Press.
4. Martin, O., & Averous, L. (2001). Poly(lactic acid): plasticization and properties of biodegradable multiphase systems. *Polymer*, 6209-6219.
5. T.H., V. E., & Steve, D. (2015). Life Cycle Inventory and Impact Assessment Data for 2014 Ingeo Polylactide Production. *Industrial Biotechnology*, 167-180.
6. Salamone, J. C. (1996). *Polymeric Materials Encyclopedia, Volume 2 C.* CRC Press.
7. Celzard, A., Mareche, J. F., Payot, F., & Furdin, G. (2002). Carbon 40 (2002) 2801–2815 Electrical conductivity of carbonaceous powders. *Carbon*, 2801-2815.
8. Frackowiak, S., Ludwiczak, J., Leluk, K., Orzechowski, K., & Kozlowski, M. (2015). Foamed poly(lactic acid) composites with carbonaceous fillers for electromagnetic shielding. *Materials and Design 65*, 749-756.
9. Choy, T. C. (1999). *Effective Medium Theory: Principles and Applications.* Oxford University Press.
10. Mclachlan, D. S., Blaszkiewicz, M., & Newham, R. E. (1990). Electrical Resistivity of Composites. *Journal of the American Ceramic Society*, 2187-2203.
11. Malte H. G. Wichmann, Buschhorn, S. T., Gehrmann, J., & Schulte, K. (2009). Piezoresistive response of epoxy composites with carbon nanoparticles under tensile load.
12. Zhang , J., Feng, S., & Wang, Z. (2004). DC Current Voltage Characteristics of Silicone Rubber. *Wiley InterScience*.
13. Sau, K. P., Chaki, T. K., & Khastgir, D. (1997). The change in conductivity of a rubber-carbon black composite subjected to different modes of pre_strain. *Elsevier*.
14. Li, L., Sun, Q., Bellehumeur, C., & Gu, P. (2002). Composite Modeling and Analysis for Fabrication of FDM Prototypes with Locally Controlled Properties. *Journal of Manufacturing Processes*, 129-141.
15. Li, L., Sun, Q., Bellehumeur, C., & Gu, P. (2002). Investigation of Bond Formation in FDM Process. *Solid Freeform Fabrication Symposium*, (pp. 1-8). Austin, TX.

16. Li, L., Sun, Q., Bellehumeur, C., & Gu, P. (2004). Modeling of Bond Formation Between Polymer Filaments in the Fused Deposition Modeling Process. *Journal of Manufactured Processes*, 170-178.

17. Rodrı´guez, J. F., Thomas, J. P., & Renaud, J. E. (2003). Mechanical behavior of acrylonitrile butadiene styrene fused deposition materials modeling. *Rapid Prototyping Journal*, 219–230.

18. Sood, A. K., Ohdar, R. K., & Mahapatra, S. S. (2011). Experimental investigation and empirical modelling of FDM process for compressive strength improvement. *Journal of Advanced Research*, 81-90.

19. Nikzad, M., Masood, S. H., & Sbarski, I. (2011). Thermo-mechanical properties of a highly filled polymeric composites for Fused Deposition Modeling. *Materials & Design*, 3448-3456.

20. Nikzad, M., Masood, S. H., Sbarski, I., & Groth, A. (2009). A Study of Melt Flow Analysis of an ABS-Iron Composite. *Tsinghua Science and Technology*, 29-37.

21. Pegel, S., Po¨tschke, P., Petzold, G., Alig, I., Dudkin, S. M., & Lellinger, D. (2008). Dispersion, agglomeration, and network formation of multiwalled carbon nanotubes in polycarbonate melts. *Polymer*, 974-984.

22. Pegel, S., Po¨tschke, P., Petzold, G., Alig, I., Dudkin, S. M., & Lellinger, D. (2008). Influence of injection molding parameters on the electrical resistivity of polycarbonate filled with multi-walled carbon nanotubes. *Composites Science and Technology*, 777-789.

23. Cabot Corporation. (2015, March). *Datasheet: Vulcan(R) XC72 Conductive Carbon Black.* (NatureWorks, LLC., 2015)

24. NatureWorks, LLC. (2015, May). *Ingeo(TM) Biopolymer 4043D Technical Data Sheet.* Retrieved from http://www.natureworksllc.com/~/media/Technical_Resources/Technical_Data_Sheets/TechnicalDataSheet_4043D_films_pdf.pdf

25. ASTM D991-89(2014), Standard Test Method for Rubber Property—Volume Resistivity Of Electrically Conductive and Antistatic Products, ASTM International, West Conshohocken, PA, 2014, www.astm.org